ICSV14
Cairns • Australia
9-12 July, 2007

14th International Congress on Sound & Vibration

A NUMERICAL STUDY OF FLUID FLOW PAST A CIRCULAR CYLINDER AT RE=3900 AND A PRACTICAL APPROACH TO NOISE PREDICTION

A. Pradera[1], G. Keith[2], F. Jacobsen[3], N. Gil-Negrete[1] and A. Rivas[4]

[1] CEIT and Tecnun (University of Navarra) - Manuel de Lardizábal 15, 20018, San Sebastián, Spain
[2] Odegaard & Danneskiold-Samsoe A/S - Titangade 15, 2200 Copenhagen N, Denmark
[3] Acoustic Technology, DTU - Building 352, 2800 Lyngby, Denmark
[4] Tecnun (University of Navarra) - Manuel de Lardizábal 13, 20018, San Sebastián, Spain
apradera@ceit.es

Abstract

The aim of this study is the prediction of the aerodynamic noise generated by the fluid flow past a circular cylinder at Re=3900, combining numerical simulation of the fluid flow with an analytical noise evaluation. This case has been extended to the flow around a cylinder with Re=140000. The Large Eddy Simulation (LES) turbulence model of FLUENT v6.3 is used in a numerical simulation of the fluid flow. The computations are carried out with double precision and second-order implicit unsteady formulation. First and second order statistics, as well as drag, lift and pressure coefficients obtained in the Computational Fluid Dynamics (CFD) calculations are in good agreement with numerical and experimental data from literature. Once the CFD simulation is validated, an approach to make noise predictions on the basis of CFD simulations is demonstrated. This approach involves deriving analytical expressions describing the relationship between certain statistical flow quantities and the far field acoustic power and is intended to circumvent the potential introduction of large errors that can arise when working directly with pressure and velocity time series. The method is here demonstrated in a very simple example and the obtained Sound Pressure Level (SPL) is compared with numerical and experimental results from the ESPRIT project ALESSIA and also with the SPL derived from the Phillips correlation.

1. INTRODUCTION

The majority of methods for predicting aerodynamic noise based on CFD calculations are predicated on one or other acoustic analogy formulation (e.g. Lighthill, Lilley, Howe). These provide a method of synthesizing an acoustic source distribution from flow data derived from the CFD results. These source data may then be applied directly in a number of acoustic solvers. This approach has many advantages, not least flexibility. Nonetheless, the direct use of point-wise surface pressure or velocity time histories (whether in the time or frequency domain and whether acquired directly or through stochastic synthesis) has severe drawbacks in practical applications. CFD methodology is typically validated (indeed calibrated) through the comparison of certain statistical averages with experiment. A method based on detailed time histories of pressure and velocity makes enormous, and in some cases unreasonable, demands on the accuracy of the simulation and introduces the possibility of large errors. Furthermore such methods have a significant overhead in storage and data transfer.

An alternative, parallel approach is outlined and demonstrated in this paper. Essentially, rather than working directly with a large number of pressure and velocity time histories, the method is based on establishing a relationship between certain flow statistics and the far field acoustic intensity under certain simplifying assumptions. CFD is much better equipped to provide these flow statistics and the reproducibility, reliability and indeed accuracy of the prediction is much improved at the expense of flexibility.

In this paper a very simple example is given in which the far field acoustic power generated by low Mach number flow past a circular cylinder is predicted from the lift coefficient calculated using CFD. Future work will show how the method may be developed to accommodate higher Mach numbers and more complex geometries.

As the low Reynolds number case gives a very low SPL, the high Reynolds number case will be studied in more detail.

2. FLOW PAST A CIRCULAR CYLINDER AT RE=3900

The CFD simulation of the flow around a cylinder at Re=3900 is shown in this section. The results are compared both with numerical simulations and experiments from the literature.

2.1 Computational details

The computational domain used to simulate the flow around a circular cylinder with a diameter *D* of 0.022 m is shown in Figure 1. The length of the domain in the streamwise *x*-direction is 27*D*, with the centre of the cylinder placed 4.5*D* downstream from the inlet; while in the lateral *y*-direction it is 9*D* long. A spanwise extent of the domain of *L = 2.3D* has been considered. A uniform grid distribution has been set along both the lateral (*y*) and spanwise (*z*) directions, with 60 and 15 elements respectively. In the radial direction around the cylinder, 50 elements have been distributed according to a geometric ratio of 1.13, which allows a reduction of the element size when getting closer to the cylinder. This grid distribution leads to a mesh of 270000 hexahedral elements.

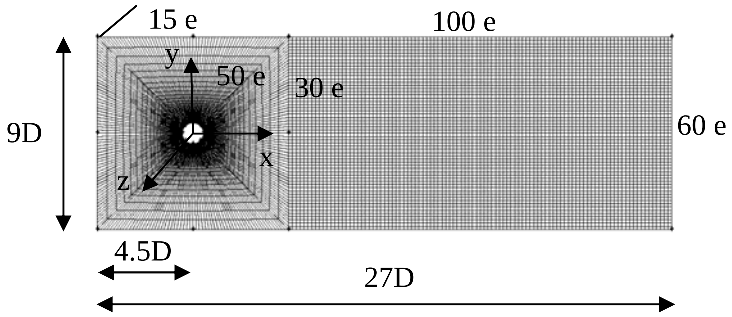

Figure 1. Computational domain.

The fluid considered in the simulation is air with a density of 1 kg/m^3 and a dynamic viscosity of 10^{-5} kg/ms. Considering a Reynolds number of Re=3900, the average speed of the flow can be calculated as:

$$U_\infty = \frac{\mathrm{Re}\cdot\mu}{D\cdot\rho} = \frac{3900\cdot 1\cdot 10^{-5}\ \mathrm{kg/m\,s}}{0.022\ \mathrm{m}\cdot 1\ \mathrm{kg/m^3}} = 1.7727\ \mathrm{m/s} \tag{1}$$

A velocity inlet boundary condition with a uniform unperturbed streamwise velocity profile of 1.7727 m/s has been set at the upwind of the domain, *x* = -4.5*D*, whereas an outflow boundary condition is assumed at the outlet (downwind) section, *x* = 22.5*D*. Periodic boundary conditions have been specified in the spanwise *z*-direction, i.e. *z* = -1.15*D* and *z* = 1.15*D*; and symmetry planes have been set on the lateral surfaces, i.e. y = -4.5D and y = 4.5D. A non-slip wall boundary condition has been specified on the cylinder surface.

A Large Eddy Simulation (LES) turbulence model has been considered, assuming the Smagorinsky-Lilly subgrid-scale model with a constant of C_S = 0.1. A maximum wall y^+ (wall-adjacent cell's centroid placement) of y^+ = 0.7464 is obtained on the cylinder wall, which shows that the grid resolution considered around the cylinder is adequate.

2.2 Statistical sampling and computational costs

A time step of $\Delta t = 10^{-4}$ s is assumed in the LES simulation. After the steady Reynolds-Averaged Navier-Stokes (RANS) simulation considering the RNG (renormalization group) based k-ε turbulence model, the LES simulation has been run during 56 vortex shedding cycles before starting the statistical averaging. The time average (mean) of the instantaneous values and the root-mean-squares of the fluctuating values have been sampled each time step during 20 shedding cycles. A Pentium (R) 4 CPU, 3.00 GHz, 2.00 GB of RAM has been used for the following steps of the simulation, with a total time of 36 days (2 hours per 100 time steps).

2.3 First and second order statistics

The flow unsteady statistics have been sampled during 20 vortex shedding cycles. Table 1 shows some characteristic flow parameters, such as the drag coefficient C_D, the base pressure coefficient C_{Pb}, the separation angle θ_{sep}, the length of the mean recirculation region L_r/D, and the Strouhal shedding frequency St.

Table 1. Mean flow parameters from DNS, LES and experiments, Re=3900.

Data from	C_D	C_{Pb}	θ_{sep}	L_r/D	St
Exp – from [1]–[2]	0.99±0.05	-0.88±0.05	86±2	1.4±0.1	0.215±0.005
DNS [3]	-	-0.96	-	1.12	0.203
DNS [4]	1.03	-0.93	85.7	1.30	0.220
LES [2]	1.04	-0.94	88.0	1.35	0.210
LES1 [4]	1.14	-0.99	87.3	1.04	0.210
LES2 [4]	1.31	-1.13	90.0	0.81	0.210
Present LES	1.4	-1.15	90.0	0.88	0.203

LES results have been compared with the Direct Numerical Simulation (DNS) of Ma et al. [3], LES of Kravchenko and Moin [2], DNS and two LES of Tremblay [4] and experimental data. The separation angle and the shedding frequency are in good agreement. The drag coefficient and base pressure coefficient are overpredicted, while the length of recirculation region, L_r, is underpredicted.

Figure 2 shows the mean streamwise velocity profile sampled along the vertical coordinate as a function of the normalized lateral distance. The profiles have been taken in the central plane z = 0.025 at various downstream distances of x/D = 1.06, 1.54, 2.02, 3.0, 4.0 and 5.0. Ma et al. [3] pointed out that both a small spanwise computational domain and a high dissipation LES favour U-shape streamwise velocity profiles, rather than V-shape profiles in the near wake. The LES studied in this paper predicts a pronounced V-shape profile in the near-wake, x/D = 1.06, according to the Particle Image Velocimetry (PIV) experiments of Lourenco and Shih [5]. Figure 3 shows the vertical profiles of the mean lateral (vertical) velocity taken at the same positions as described above. Good agreement is observed both for mean streamwise and vertical velocity profiles. The vertical profiles of the streamwise velocity fluctuations are shown in Figure 4. The overall agreement with the experimental and numerical data is quite acceptable, although LES predicts higher peaks in the near wake, that is, *x/D* = 1.06. At *x/D* = 3.0 and *x/D* = 4.0 LES results agree better with the experimental data in the ESPRIT project ALESSIA [6].

Figure 5 shows vertical profiles of lateral (vertical) velocity fluctuations. LES leads to higher peaks in the near wake, but very good agreement is observed downstream. Figure 6 shows the mean streamwise velocity in the centreline of the cylinder (a), as well as the pressure coefficient on the cylinder surface (b). The maximum backflow velocity predicted by the LES simulation agrees quite well with the experiment of Ong and Wallace [7]. The recirculation length L_r is underpredicted by the LES simulation, as shown in Table 1. The distribution of the pressure coefficient along the cylinder surface shows a lower value compared with the experiment of Norberg [8], especially in the rear of the cylinder.

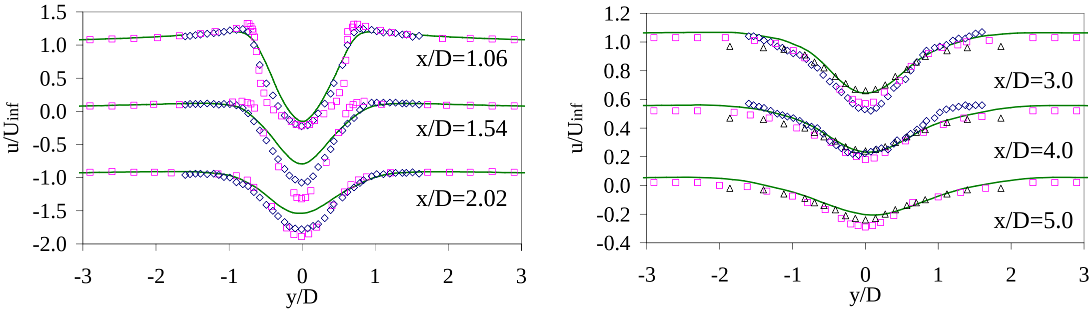

Figure 2. Vertical profiles of mean streamwise velocity: LES (—), LES Kravchenko & Moin (□) [1]-[2], exp. Lourenco & Shih (◊) [5], exp. in ALESSIA (Δ) [6].

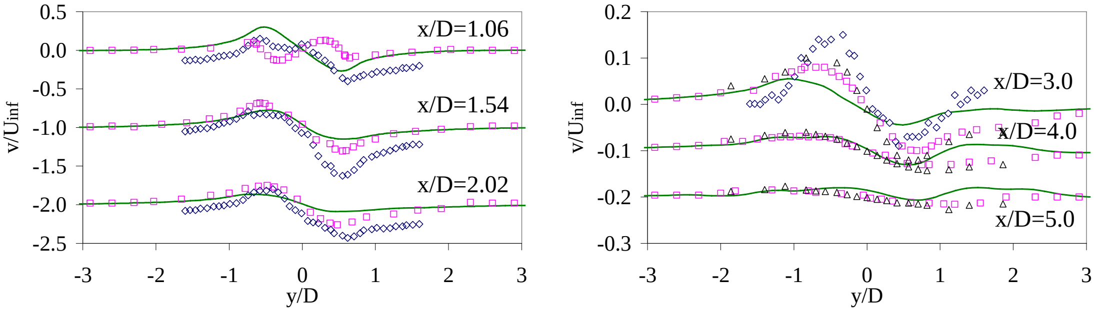

Figure 3. Vertical profiles of mean lateral (vertical) velocity. Symbols as in Figure 2.

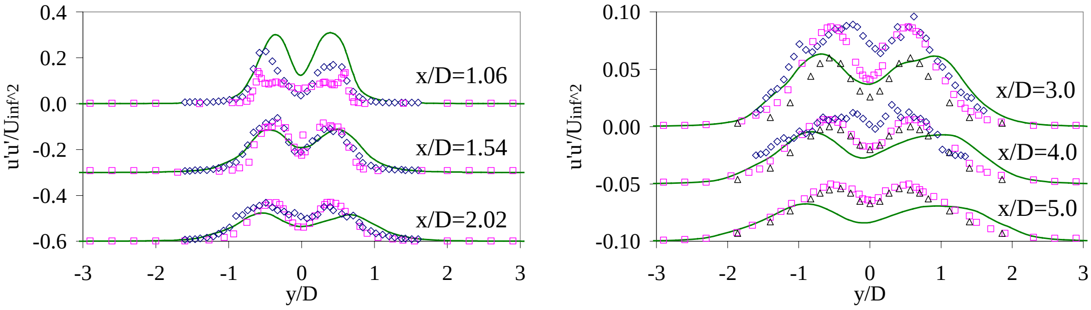

Figure 4. Vertical profiles of streamwise velocity fluctuations. Symbols as in Figure 2.

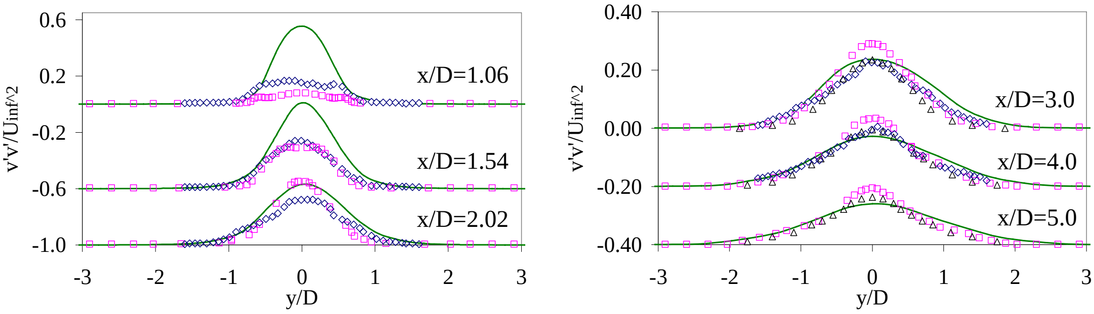

Figure 5. Vertical profiles of lateral (vertical) velocity fluctuations. Symbols as in Figure 2.

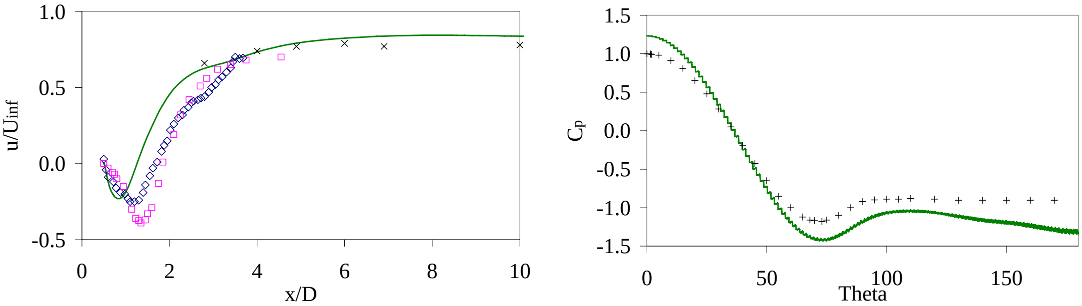

Figure 6. (a) Mean streamwise velocity; (b) Pressure Coefficient. Symbols: LES (—), LES Kravchenko & Moin (□) [1]-[2], exp. Lourenco & Shih (◊) [5], exp. Ong & Wallace (×) [7], exp. Norberg (+) [8].

3. FLOW PAST A CIRCULAR CYLINDER AT RE=140000

In this section the LES computation of the flow around a circular cylinder at Re=140000 is presented and compared with the experiment of Cantwell and Coles [9].

3.1 Computational details

The computational domain used to simulate the flow around a circular cylinder at Re=140000 has the same dimensions as in the Re=3900 case, differing only with respect to the cylinder diameter D, which is 0.04 m. A uniform grid distribution has been set along both the lateral (y) and spanwise (z) directions, with 60 and 30 elements respectively. In the radial direction around the cylinder, 50 elements have been distributed according to a geometric ratio of 1.13. After the square with a finer mesh around the cylinder, 150 elements have been set in the streamwise x-direction. This grid distribution leads to a mesh of 630000 hexahedral elements.

A velocity inlet boundary condition with a uniform unperturbed streamwise velocity profile of 35m/s has been set at the upwind of the domain. The remaining boundary conditions are the same as in the Re=3900 case. LES turbulence model has been used.

3.2 Statistical sampling and computational costs

A time step of Δt = 10^{-5} s is assumed. After the RANS simulation considering $k-\varepsilon$ RNG viscous model, the LES simulation has been run during 60 vortex shedding cycles before starting the statistical averaging. The time average (mean) of the instantaneous values and the root-mean-squares of the fluctuating values have been sampled during 20 shedding cycles. Samples of each of time step have been taken into account. A Pentium (R) 4 CPU, 3.00 GHz, 2.00 GB of RAM has been used for the following steps of the simulation, with a total time of 42 days (2.5 hours per 100 time steps).

3.3 First and second order statistics

The flow unsteady statistics have been sampled during 20 vortex shedding cycles. Table 2 shows the drag coefficient C_D, the base pressure coefficient C_{Pb}, the separation angle θ_{sep}, the length of the mean recirculation region L_r/D and the Strouhal number St. LES results have been compared with results of Travin et al. [10], Breuer [11] and Tremblay [4], and experimental data of Cantwell and Coles [9]. LES results are within the range predicted by DES, except the separation angle, which is overpredicted; but differ from the experimental data. The Strouhal number predicted by LES is higher than the Strouhal number measured by Cantwell and Coles [9], who point out that the present value is slightly lower than the consensus of other experiments.

Figure 7 shows the vertical profiles of mean streamwise velocity at two different positions downstream. Good agreement with the experimental data can be observed. Figure 8 shows the profile of the mean lateral velocity. Quite good results are obtained; although sampling data in more vortex shedding cycles would help to a better agreement.

Table 2. Mean flow parameters from DES, LES and experiments, Re=140000.

Data from	C_D	C_{Pb}	θ_{sep}	L_r/D	St
Exp [9]	1.237	-1.21	77	0.44	0.179
DES [10]	0.87, 1.08	-0.81, -1.04	77, 78	1.1, 1.5	-
LES [11]	1.22, 1.45	-1.40, -1.76	92.6, 96.4	0.34, 0.57	-
LES H1 [4]	1.134	-1.22	90	0.98	-
LES H2 [4]	0.937	-0.980	90	1.47	-
LES H3 [4]	1.27	-1.45	96.7	0.44	-
Present LES	0.892	-0.857	92.0	1.05	0.234

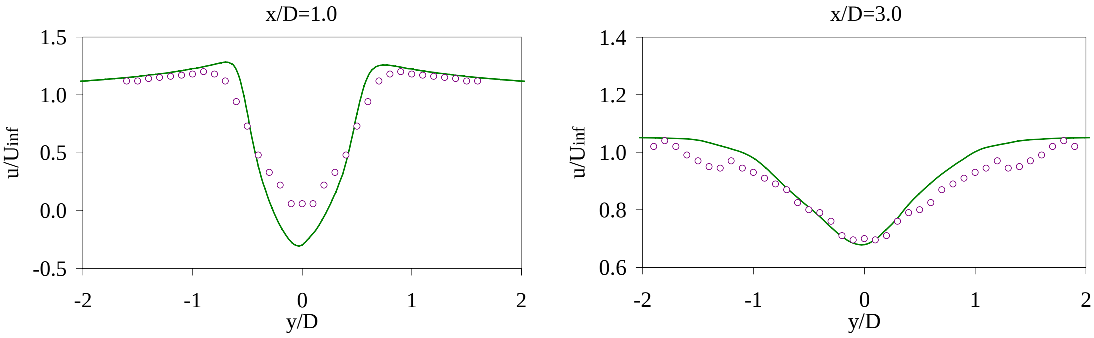

Figure 7. Vertical profiles of mean streamwise velocity: LES (—), exp. of Cantwell and Coles (o) [9].

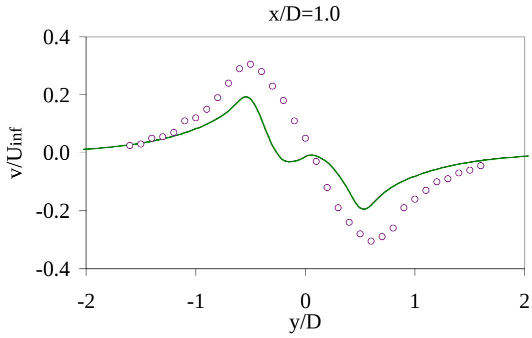

Figure 8. Vertical profiles of mean lateral (vertical) velocity. Symbols as in Figure 7.

Figure 9 shows the RMS values of streamwise (a) and crossflow (b) velocity fluctuations along the centreline of the cylinder. Although a lower value is predicted in both cases, quite fair agreement is observed. Whereas Breuer [11] and Tremblay [4] show a higher peak for v', LES predicts a lower peak value, but closer to the measurements. Figure 10 shows the mean streamwise velocity (a) and the pressure coefficient (b). Both the recirculation length L_r and the base pressure coefficient are underpredicted.

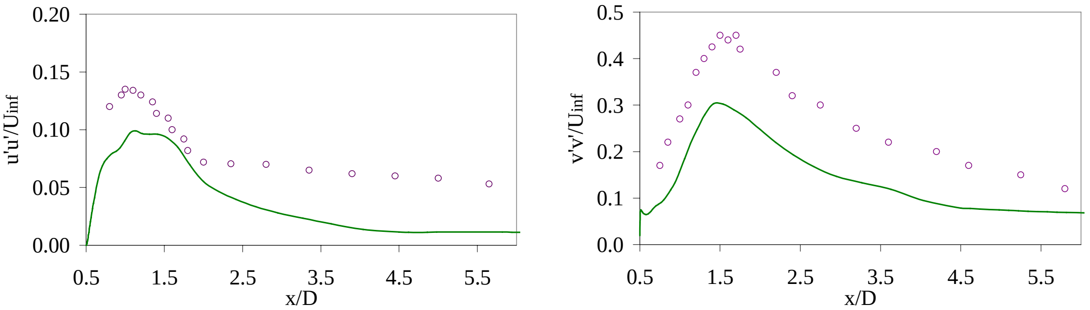

Figure 9. (a) Vertical profile of streamwise velocity fluctuations; (b) Vertical profiles of lateral (vertical) velocity fluctuations. Symbols as in Figure 7.

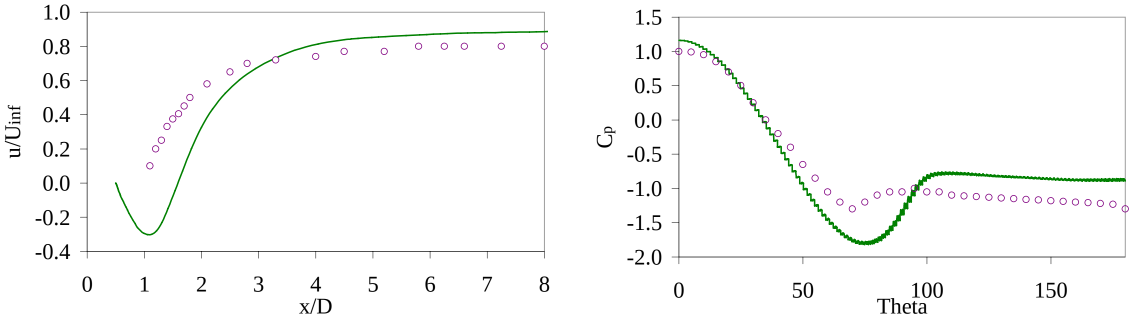

Figure 10. (a) Mean streamwise velocity; (b) Pressure Coefficient. Symbols as in Figure 7.

4. ANALYTICAL NOISE PREDICTION

With the lift coefficient obtained from the CFD simulation as input, the total sound power radiated to the far field can be obtained from expressions given in [13] in the following dimensionless form:

$$\pi\left(\frac{L}{D}, Re, Ma, St\right) = \frac{P}{\rho U^3 LD} = \frac{1}{48\pi} Ma^3 St^2 \frac{L}{D} C_L^2(Re, St) \qquad (2)$$

where P is the total power, ρ is the density, U is the flow speed, L and D the length and diameter of the cylinder respectively, $Ma=U/c$ is the Mach number, $St=\omega D/U$ is the Strouhal number and C_L^2 is the lift coefficient (power) acting on the cylinder in function of the Reynolds and Strouhal numbers. As lower Reynolds number case gives a very low sound pressure level, near the threshold of hearing, only the noise prediction of Re=140000 is analysed in detail. The overall sound pressure level (OASPL) obtained by our method is compared with numerical results and Philips equation [14] in Table 3. Phillips' method predicts the OASPL determining all the flow parameters from measurements, whereas the approach presented in this paper considers the flow parameters from the CFD. Very good agreement is obtained with Phillips correlation result. As shown by Montavon [12], the Phillips correlation results agree very well with the measurements, therefore the analytical prediction agrees also with experimental measurements.

Table 3. Overall Sound Pressure Level.

	Analytical Scaled	Montavon Numerical [12]	Montavon (from Phillips) [12]
OASPL(dB)	96.2	100.3	95.8

Figure 11 compares the predicted sound pressure level (SPL) frequency spectrum (a) and that obtained by Montavon [12] (b) for the same resolution, at a distance of 1m from the cylinder. The two cases differ a little in the geometry, so our results have been extrapolated to the dimensions of the Montavon case from the dimensionless form given in equation (2).

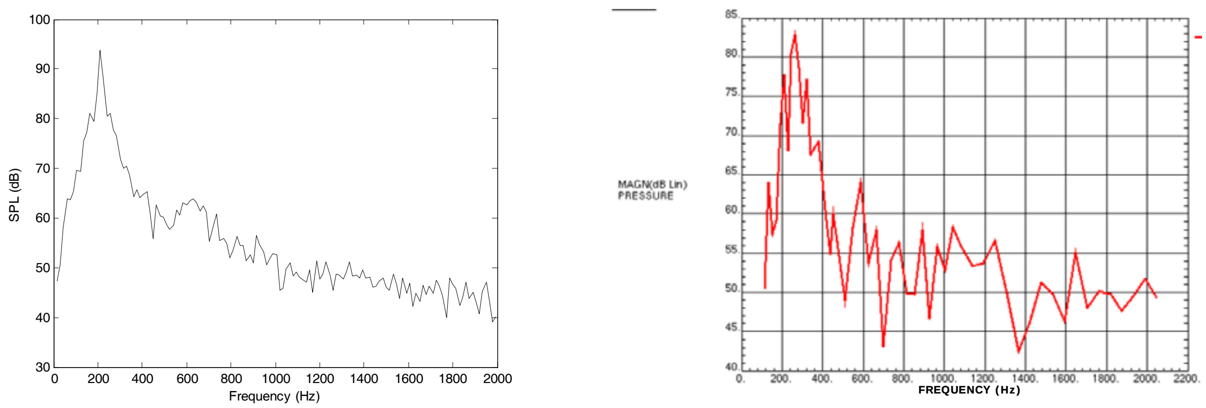

Figure 11. Sound Pressure Level frequency spectrum, Re=140000. (a) Predicted; (b) Numerical [12].

5. CONCLUSIONS

The approach outlined in the introduction gives excellent results in this simple case. Future work will investigate ways in which the approximations inherent in equation (2) may be rolled back to give expressions for higher Mach number and more complex geometries. The approach will be extended to further application cases, including a high-speed train pantograph, a valve and a backward-facing step.

ACKNOWLEDGMENTS

This research work is supported by a Marie Curie Grant from the European Doctorate in Sound and Vibration Studies (EDSVS).

REFERENCES

[1] A. G. Kravchenko and P. Moin, *B-spline methods and zonal grids or numerical simulations of turbulent flows*, Report No. TF-73, Flow Physics and Computation Division, Department of Mechanical Engineering, Stanford University, 1998.

[2] A. G. Kravchenko and P. Moin, "Numerical studies of flow over a circular cylinder at Re_D = 3900", *Physics of Fluids* **12**, 403-417 (2000).

[3] X. Ma, G-S. Karamanos, and G. E. Karniadakis, "Dynamics and low-dimensionality of a turbulent near wake", *Journal of Fluid Mechanics* **410**, 29-65 (2000).

[4] F. Tremblay, Direct and large-eddy simulation of flow around a circular cylinder at subcritical Reynolds numbers, PhD thesis, Technical University of Munich, 2001.

[5] L.M. Lourenco and C. Shih, *Characteristics of the plane turbulent near wake of a circular cylinder. A particle image velocimetry study*, private communication, 1993. Data taken from [1].

[6] ESPRIT project ALESSIA, Application of large-eddy simulation to the solution of industrial problems.

[7] J. Ong and L. Wallace, "The velocity field of the turbulent very near wake of a circular cylinder", *Experiments in Fluids* **20**, 441-453 (1996).

[8] C. Norberg, "Pressure forces on a circular cylinder in cross flow". In H. Eckelmann, J. M. R. Graham, P. Huerre and P. A. Monkewitz, editors, *Proceedings of IUTAM Symposium on Bluff-Body Wakes, Dynamics and Instabilities*, Berlin, 1993, pp. 275-278. *IUTAM-Symposium*, Göttingen, Germany, 7-11 September 1992, Springer-Verlag.

[9] B. Cantwell and D. Coles, "An experimental study of entrainment and transport in the turbulent near wake of a circular cylinder", *Journal of Fluid Mechanics* **136**, 321-274 (1983).

[10] A. Travin, M. Shur, M. Strelets, and P. Spalart, "Detached-eddy simulations past a circular cylinder", *Flow, Turbulence and Combustion* **63**, 293-313 (2000).

[11] M. Breuer, "A challenging test case for large eddy simulation: high Reynolds number circular cylinder flow", *International Journal of Heat and Fluid Flow* **21**, 648-654 (2000).

[12] C. Montavon et al., "Noise propagation from a cylinder in a cross flow: comparison of SPL from measurements and from a CAA method based on a generalized acoustic analogy", *IMA Conference on Computational Aeroacoustics*, 9-11 April 2002, University of Greenwich – Maritime Greenwich Campus.

[13] D.G. Crighton, A.P. Dowling, J.E. Ffowcs-Williams, M. Heckl and F.G. Leppington, *Modern Methods in Analytical Acoustics*, Springer-Verlag, London, 1992.

[14] O.M. Phillips, "The intensity of Aeolian Tones", *Journal of Fluid Mechanics* **1**, 607–624 (1956).